LANDYNE 蓝带软件

User Manual

CTFscope

Simulation and visualization of contrast transfer function for

conventional and aberration corrected TEM

Table of contents

1. Introduction

For the characterization of novel materials such as ceramics, metal alloys, semiconductor systems, high-T_c superconductors, and structural study on biomaterials, one needs to have high-resolution transmission electron microscope (HRTEM) images with an interpretable resolution down to the atomic level. The application of TEM in order to obtain high-resolution information involves the problem of objective lens aberrations. If the TEM is appropriately aligned, the wave aberrations are mainly caused by the spherical aberration of the objective lens. It is clear that the irregular phase delays occurring due to lens aberration must be minimized to obtain high-resolution images.

Phase contrast transfer function or contrast transfer function (CTF) describes how aberrations in a TEM modify the image of a sample [1~5]. By considering the recorded image as a CTF-degraded object, describing the CTF allows the object to be reverse-engineered. A comprehensive understanding of the CTF is vital to analyzing high-resolution images in electron microscopy. In working on AC-TEMs, automatic correction functions do not always exhibit optimal performance. Thus, the analysis of CTF is particularly important to achieve the best resolution using the manual control mode. Apart from microscopists, the researchers and students whose works involve TEM will also be highly beneficial for the understanding of the content on the CTF.

Software programs and scripts for simulation and visualization of CTF have been developed and available in the public domain for conventional TEM [6~8] and aberration-corrected (AC-) TEM [9]. Two programs were launched nearly twenty years ago [6,7], and the script was updated in 2017 [8]. Lee *et al*. [9] then developed the extended CTF (exCTF) simulator to perform the primary and extensive CTF calculation, designed to obtain more information than the early reported software. As inspired by the previous software on CTF, we developed the CTFscope as a simulation and visualization tool of the CTF with user-friendly interface for conventional TEM and AC-TEM. The CTFscope, as one of the components in the Landyne suite [10], can be downloaded from the website listed in the reference. It expects that the CTFscope will help

readers better understand the instrumental performance information and the effects of the aberration parameters for TEM image formation through CTF simulation and visualization.

2. Theoretical background and formulas

This section briefly describes theoretical background and the formulas used in the CTFscope for calculation. The author recommends that readers refer to the original papers and related books for more detailed information [1-5, 11-15]. Let us consider an electron transmission wave passing through a slice of sample,

$$q(x, y) = \exp\left[i\sigma\phi_p(\text{x}, \text{y})\Delta z\right] \qquad (1)$$

where σ is the interaction coefficient at the microscope accelerating voltage, $\phi_p(x, y)$ is the specimen potential projected in the direction of the incident electron beam and Δz is the specimen thickness through which the projection is taken. Under the kinematic scattering approximation, for "weak-phase-object," diffractogram intensity is then written as,

$$I(u, v) = \delta(u, v) + 2\sigma V(u, v)\,\Delta z\,sin\chi(u, v) \qquad (2)$$

where $V(u, v)$ is the Fourier coefficients of $\phi_p(\text{x}, \text{y})$ and $\sin\chi(u, v)$ is the CTF. The first and second terms of Eq. (2) correspond to the transmitted and scattered beams, respectively.

The microscope characteristic transfer function consists of the production form of four functions, namely, the objective aperture function, the CTF, the partial spatial coherence function, and the partial temporal coherence function. Considering a circular aperture with a radius R. The aperture function can be represented as simply

$$w(u, v) = \begin{cases} 1, \sqrt{u^2 + v^2} \leq R \\ 0, \quad otherwise \end{cases} \qquad (3)$$

The other three functions will be given in detail below.

2.1 The CTF for conventional TEM [11]

For conventional TEM, the $\chi(u, v)$ is given by

$$\chi(u, v) = \pi[\Delta f\lambda(u^2 + v^2) - 0.5C_s\lambda^3(u^2 + v^2)^2] \qquad (4)$$

In Eq. (4), Δf and C_s correspond to a defocus value and a spherical aberration coefficient of the objective lens, respectively, and the λ is the wavelength of the primary electrons. The astigmatic and other aberrations are considered in the next formula.

2.2 The CTF for aberration-corrected TEM [9]

For AC-TEM, the $\chi(u, v)$ is involved higher order of aberration factors. The complex coordinate $g = (u, v)$ is represented with the complex scattering angle ω simply by the relation

$$\omega = \lambda g \tag{5}$$

the λ is the one in Eq. (4). The function†

$$\chi(g) = \frac{2\pi}{\lambda} \chi'(\omega) \tag{6}$$

is a real function, because of the conservation of the phase-space volume. Using a common notation, the power series of χ in terms of $\omega = \lambda g$ and its complex conjugate $\bar{\omega}$ can be written as

$$
\begin{aligned}
\chi'(\omega) = Re \Big\{ & \frac{1}{2}\omega\bar{\omega}C_1 + \frac{1}{2}\bar{\omega}^2 A_1 + \omega^2\bar{\omega}B_2 + \frac{1}{3}\bar{\omega}^3 A_2 + \frac{1}{4}(\omega\bar{\omega})^2 C_3 \\
& + \omega^3\bar{\omega}S_3 + \frac{1}{4}\bar{\omega}^4 A_3 + \omega^3\bar{\omega}^2 B_4 + \omega^4\bar{\omega}D_4 + \frac{1}{5}\bar{\omega}^5 A_4 \\
& + \frac{1}{6}(\omega\bar{\omega})^3 C_5 + \frac{1}{6}\bar{\omega}^6 A_5 + \cdots \Big\}
\end{aligned} \tag{7}
$$

Following very old conventions, the index of each coefficient is the order of the corresponding ray aberration and not of the wave aberration. Thus, for example, the defocus Δf and the third-order spherical aberration C_s are addressed as C_1 and C_3, respectively. It is clear that Eq. (4), the formula for conventional TEM, is a simplified version of the formula above. Various label systems for aberration coefficients were used in the literature [12,13].

2.3 The CTF envelope functions [14]

The energy fluctuation of incident electrons and their convergence on the specimen deteriorate the resolution of electron microscopes. The aberration due to the fluctuation of incident electron energy is called chromatic aberration, and this causes a fluctuation of the focus in high-resolution

images. Fluctuations in both the accelerating voltage and the objective lens current contribute to the amount of focus fluctuation, *i.e.*,

$$\Delta = C_c[\left(\frac{\Delta V_r}{V_r}\right)^2 + \left(2\frac{\Delta I}{I}\right)^2 + (\frac{\Delta E}{E})^2]^{1/2}$$

(8)

where C_c is the chromatic aberration coefficient for the objective lines. $\frac{\Delta V_r}{V_r}$ is the fractional change in voltage over the time scale of image acquisition, V_r is the corrected accelerating voltage taking into account the relativistic effect on the electron mass. $\frac{\Delta I}{I}$ is the fractional change in lens current, and $\frac{\Delta E}{E}$ is the energy spread in the electron beam as a function of the total energy. The effect of damp in scattering amplitudes due to chromatic aberration, partial temporal coherence function, is given as

$$D = \exp\left(-\frac{1}{2}\pi^2\lambda^2\Delta^2(u^2 + v^2)^2\right)$$

(9)

while the effect due to beam convergence, partial spatial coherence function, is given by

$$S = \exp\left(-\pi^2\left(\frac{\alpha}{\lambda}\right)^2\left(C_s\lambda^3(u^2 + v^2)^{3/2} - \Delta f\lambda(u^2 + v^2)^{1/2}\right)^2\right)$$

(10)

where α indicates beam convergence, defined by the semi-angle subtended by the effective source at the specimen. These two functions are considered to be envelope functions that limit the contribution of the scattered electrons to high-resolution images.

2.4 The dumping envelope due to drift [15]

Only continuous drift case is considered here. Due to a steady drift, let the object move with constant velocity *v* during the exposure of length *T*.

$$x_D(t) = vt$$

(11)

The dumping envelope function can be derived with (11) as

$$M(u, v) = \frac{1}{T}\int_0^T e^{2\pi i(uV_x + vV_y)t}dt = \frac{\sin[\pi(uV_x + vV_y)T]}{\pi(uV_x + vV_y)T}$$
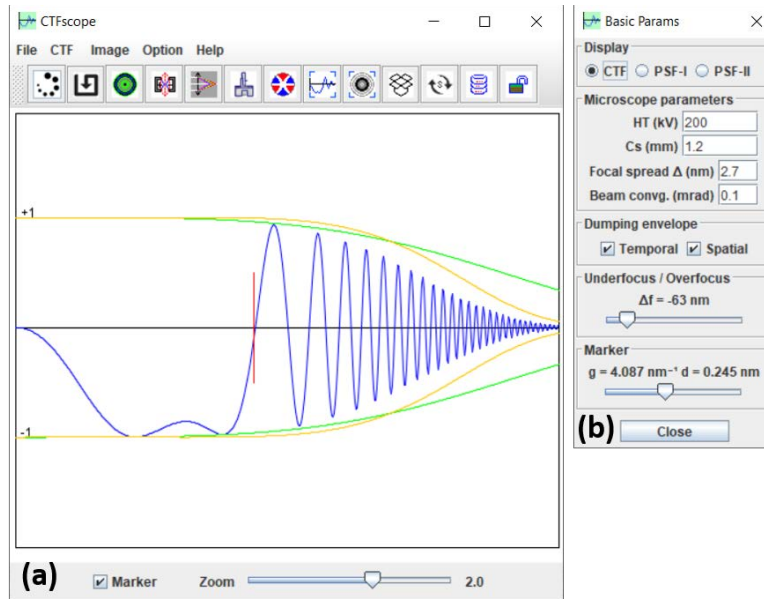
(12)

Figure 1. The main frame of the CTFscope with a graphic panel and (b) a dialogue box for microscope setup and optical parameters.

3. Design and features of the CTFscope

The CTFscope was developed with the Java programming language. The purpose of the software is to simulate and visualize CTF graphs for various TEM specifications, which can be specified close to experimental conditions for any specific TEM. The CTFscope provides users with an instant and intuitive simulation result for different instrumental and optical parameters. Both 1D and 2D graphs of the CTF are immediately calculated according to these editable parameter values. All the parameters and simulation results are displayed using a graphical user interface (GUI).

3.1 The graphic user interface

Figure 1 shows (a) the main graphical interface of the CTFscope and (b) a dialogue box of basic parameters. Users may set the instrumental parameters for a specific microscope, which can be either a commercial type or a new custom type. These parameters can be saved to or loaded from ASCII text files. The basic parameters include the high voltage, the spherical aberration coefficient C_s, the focal spread value, and the beam convergent semi-angle. The focus

value can be adjusted via a slider bar, so is a marker available for easy measurement. The chromatic aberration coefficient C_c and related parameters for calculating the focal spread value are given in a separate dialogue box in Figure 2(a). The positions and radius of an aperture and the parameters of a continuous drift are given in Figure 2(b). Astigmatism and other higher order aberration coefficients up to fifth order except S5 and R5 are provided in an additional dialogue box in Figure 2(c). Each aberration coefficient except the real coefficient C5 is controlled via two factors, the magnitude, and azimuth angle of aberration. The labels for the parameters can be switched between the two sets of well-known label systems [12, 13].
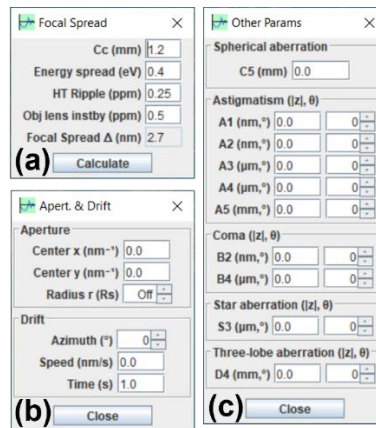

Figure 2. The dialogue boxes for (a) focal spread coefficients, (b) the parameters for an aperture and a continuous drift, (c) astigmatism coefficients, and other higher order aberration coefficients.

3.2 CTF simulation

The calculated CTF 1D and 2D graphs from the default parameters are displayed in Figure 1(a) and Figure 3. The calculation includes the envelope functions of a temporal and spatial coherence function. The 2D graph can be displayed in pseudo-color and three sets of grayscales, a pseudo color (from 0 black to -1 green and 1 blue), a grayscale I (from 0 black to $|\pm1|$ white), a grayscale II (from 0 white to $|\pm1|$ black) and a grayscale III (from -1 black to 1 white). The circular marker is in Figure 3(b ~ d).

The calculated CTF 1D and 2D graphs can be saved as images in various formats, e.g., TIFF, JPEG, PNG, and GIF. Furthermore, previously calculated results or experimental

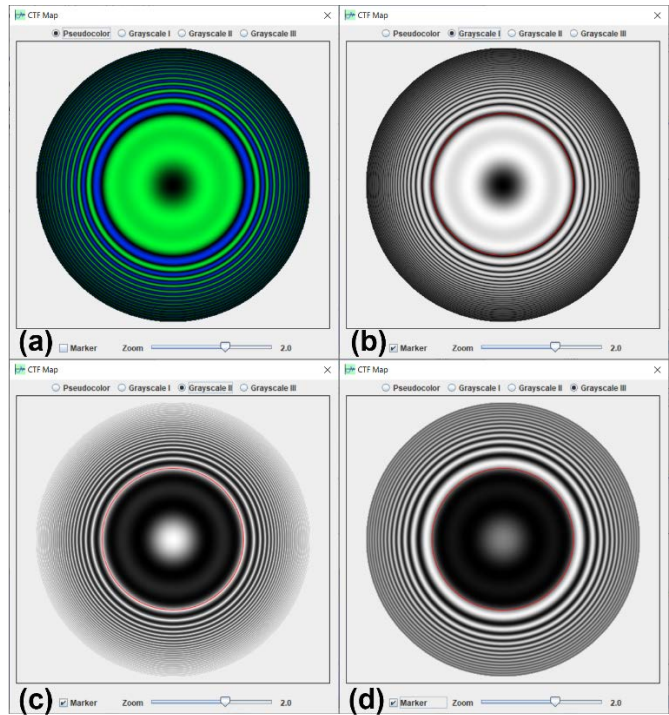diffractograms may be loaded in a separate image frame for comparison with the current CTF 2D graph.

Figure 3. The display panel for the calculated CTF in (a) a pseudo color, (b) a grayscale I (from 0 black to |±1| white), a grayscale II (from 0 white to |±1| black) and (d) a grayscale III (from -1 black to 1 white). The circular marker is in (b ~ d).
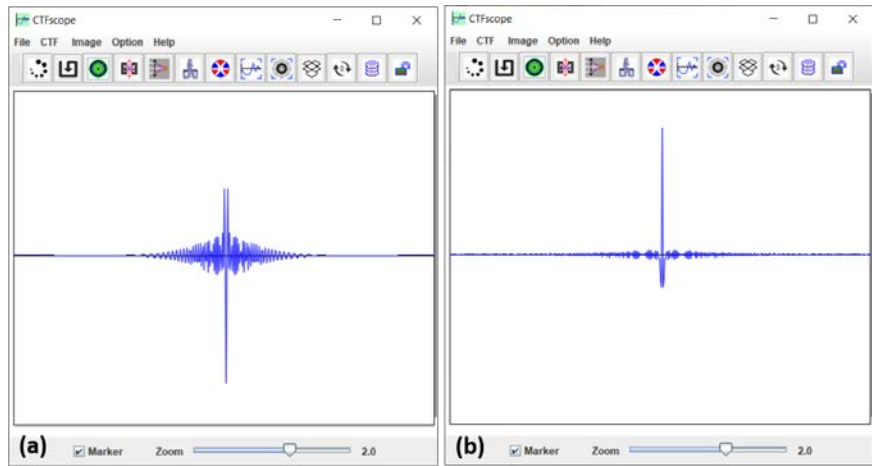

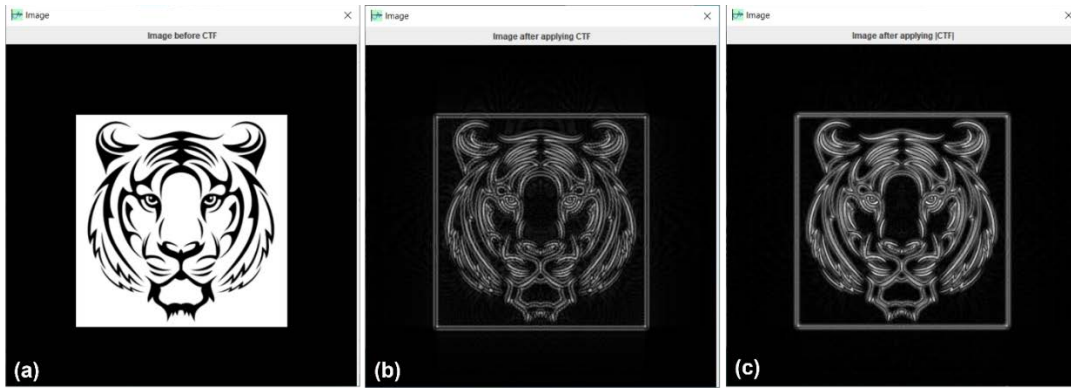Figure 4. The point spread functions as the Fourier transform of (a) the CTF and (b) |CTF|.

Figure 5. (a) An original image before processing, (b) the processed image using CTF, and (c) the processed image using |CTF|.

3.3 The image transformation

For tutorial purposes, the point spread functions are provided as the Fourier transform of the CTF and |CTF| as shown in Figure 4; an image can be loaded for processing using the two types of point spread functions in 2-dimensional mode. The example images are shown in Figure 5. The point spread function in Figure 4(b) is relatively sharper than the one in Figure 4(a), and the image in Figure 5(c) is sharper than the one in Figure 5(b). When the CTF parameters were retrieved from an amorphous area or layer, experimental HRTEM images of crystals can be enhanced using the same method and then followed by crystallographic processing. This strategy is implemented in the Simpa software in the Landyne suite [7].
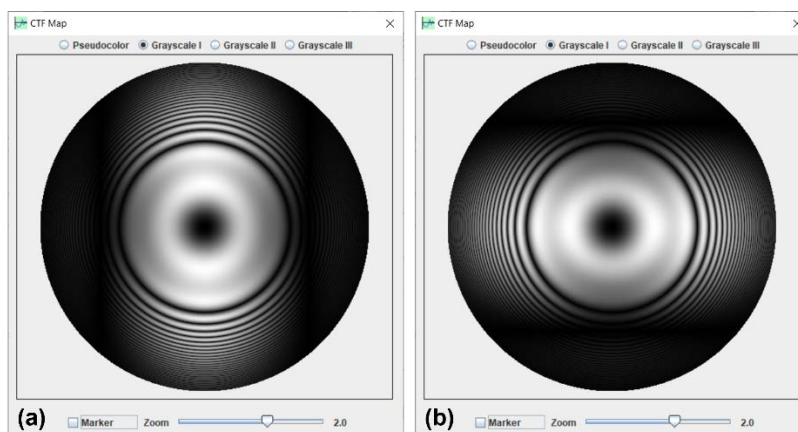

Figure 6. Two CTF 2D graphs with the continuous drift dumping effect, (a) v = 0.2 nm/s, t = 1 s and azimuth = 0⁰, and (b) v = 0.2 nm/s, t = 1 s and azimuth = 90⁰;
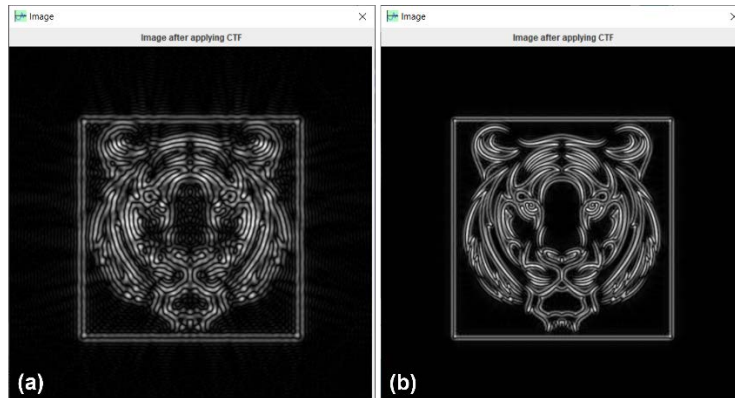
Figure 7. The processed image using a CTF with an aperture, (a) the radius as half of the Scherzer resolution, (b) the radius as one of the Scherzer resolution.

3.4 The effect of a continuous drift

Let us now consider the effect of a continuous drift as a kind of dumping envelope. Figure 6 shows two CTF 2D graphs with a continuous drift in parameters (a) v = 0.2 nm/s, t = 1 s and azimuth = 0° , and (b) v = 0.2 nm/s, t = 1 s and azimuth = 90°. Similar diffractograms of an amorphous area in TEM experiments can be seen when the sample has drifts. The drift effect on an image can also be simulated by applying the CTF on the load image (not shown).

The effect of the aperture on the image is shown in Figure 7. When a small aperture, e.g., a radius in half of the Scherzer resolution, is used, the image in Figure 7(a) is blurred. When an aperture, e.g., radius in the Scherzer resolution, is used, the image in Figure 7(b) is comparable to the one in 4(c).

4. **Usage of the CTFscope**

Usage of the CTFscope is straightforward. As shown in Figure 1(b) andFigure 2, the parameters are divided into four dialogue boxes, (i) primary data for CTF calculation; (ii) the complement data for the first dialogue box; (iii) the parameters to describe the aperture and the drift effects; (iv) higher order aberration coefficients for AC-TEM. When the parameters are updated, the

11

CTF, PSF-I, and PSF-II curves are automatically renewed. Dumping envelope curves can be displayed as an option. The aperture and the drift effect can also be regarded as dumping envelopes. The CTF 1D and 2D graphs can zoom in and out separately. A marker is available to the CTF curve for measurement. The marker can also be applied to the 2D graph only when the same zoom in the 1D graph. An image can be loaded for comparison or as a sample image to make CTF and |CTF| transformations. All parameters can be saved to a file and reloaded. Scherzer focus can be calculated directly from the drop-down menu and applied to the focus slider. The CTF 1D and 2D graphs can be saved to a file in various formats, e.g., TIFF, JPEG, PNG, and GIF. Examples were given in the previous section, where the default values were used in the calculation. These examples can be viewed as a brief guideline to the CTFscope. The following two applications are related to the figures in the published papers [9, 12].

5. Application examples

5.1 Example 1

The first example is to compare the calculated 2D graphs with experimental diffractograms in Figure 1 of reference [9]. The diffractograms were taken from a standard 200 kV Philips CM200ST microscope, which was equipped with a field emission gun with C_s =1290 µm.
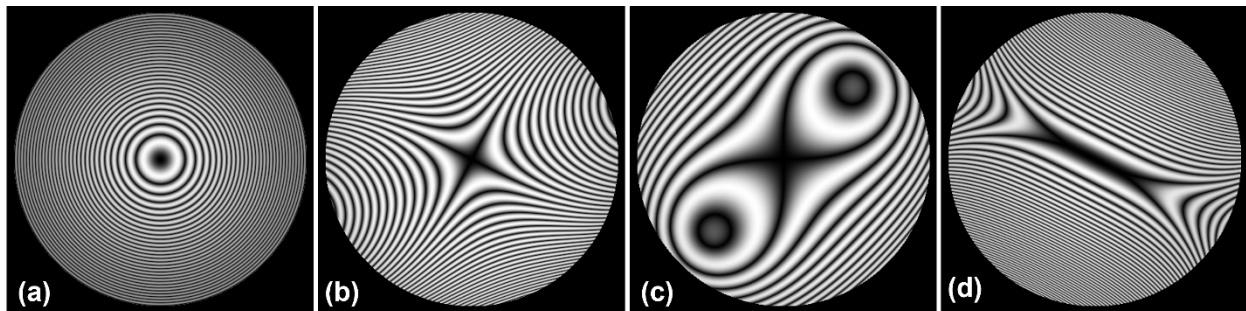

Figure 8. The calculated images using the same parameters in Figure 1 of reference [9].

Figure 8 shows calculated CFT 2D graphs using the same parameters as those in Figure 1 of the reference [9], (a) C_1 = -633 nm, A_1 = 0; (b) C_1 = 0, A_1 = 308 nm / -144°; (c) C_1 = 0, A_1 = 85 nm / -88°; (d) C_1 = -404 nm, A_1 = 400 nm / -53°. The calculated images match well to the

experimental diffractograms except for the central region, which is dark in the calculated graphs while bright in the diffractogram.
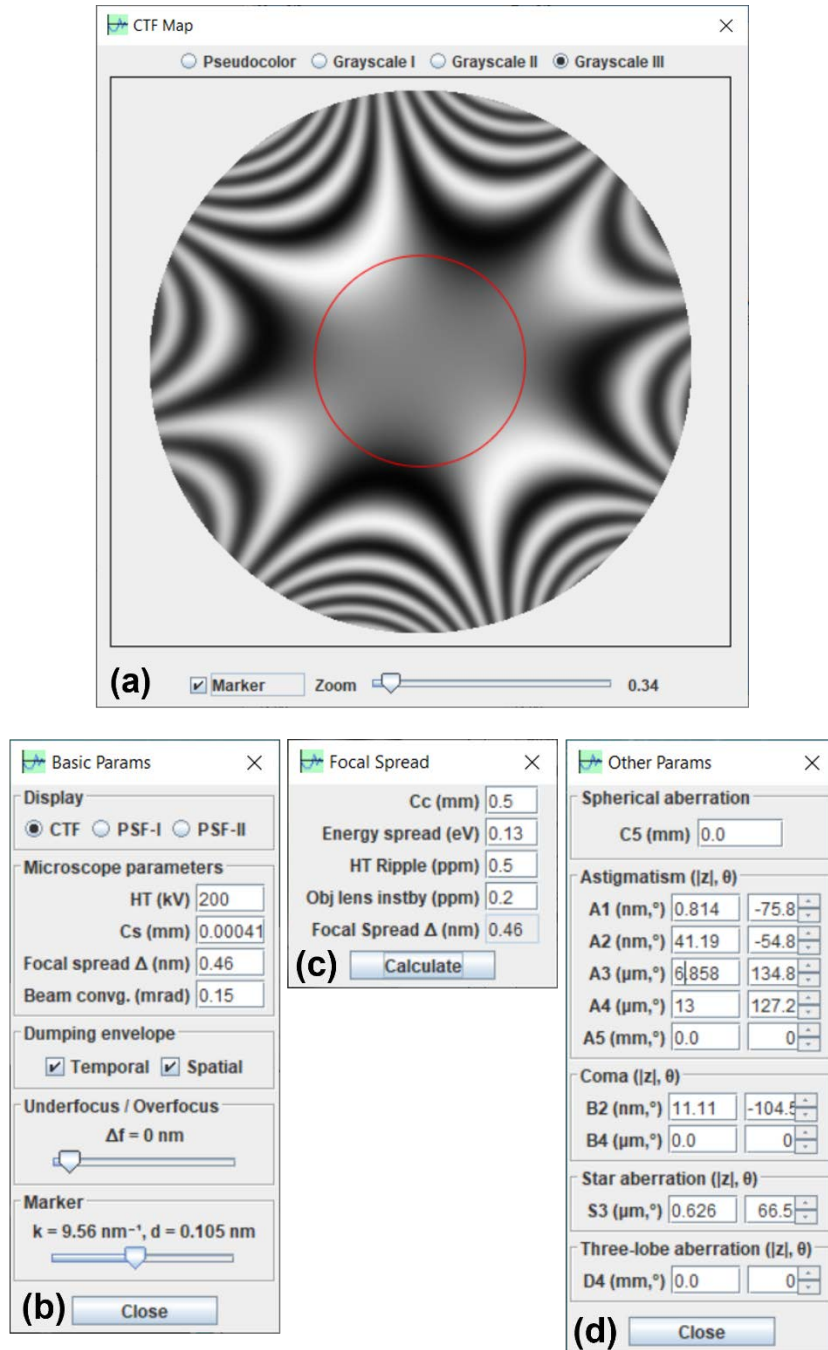

Figure 9. (a) The CTF 2D graph without aperture and drift, calculated using CTFscope using (b-d) the same parameters as those in Figure 4 of reference [12].

5.2 Example 2

The second example is to compare the calculated results by CTFscope with other software, e.g., exCTF. Figure 4 of reference [12] was calculated based on experimental data obtained from an AC-TEM device and compared to a calculated image from the commercial GUI program (CETCOR, CEOS). Figure 9 (a) shows a CTF 2D graph calculated using CTFscope with (b) the same aberration parameters in Figure 4 of reference [12]. One point needs to be pointed out that different grayscale is used in the CTF 2D graphs. Most CTF 2D graphs using grayscale I (0 = black; both 1 and -1 = white), Figure 9(a) and the CTF graphs by exCTF using grayscale III (-1 = black and 1 = white). The agreement among these CTF 2D graphs is confirmed that the CTFscope can provide accurate calculation and visualization results for various TEM devices.

6. Installation of the Landyne suite

The CTFscope is one of the key components in the Landyne software suite, which can be download from the Landyne website:

https://landyne.com

Decompress the installation file landyne.z7 in a folder, for example, c:\landyne5\. It includes a set of sub-folders, the documents folder contains user manuals for all software, including this one, and the programs folder contains executable files. For convenience, it is recommended to create a shortcut to landyne.exe and move it to the desktop. To start the launcher by double clicking on landyne.exe.

The Landyne suite requires Java Runtime Environment above JRE 1.8.0. The image TIFF format needs the support of Java Advance Image, for example, JAI-1_1_3-LIB.zip , which can be downloaded online, e.g.,

https://www.unl.edu/ncmn-enif/xzli/download/.

After decompression, copy jai_core.jar and jai_codec.jar to the JRE folder of the Java system of the microcomputer, for example, c:\program files\java\jre1.8.0_31\lib\ext\.

[†] In Eqs. (6) and (7), the letters are used slightly different with reference [12], in order to keep the consistent with Eqs. (2) and (4).

7. References

[1] DB Williams, CB Carter, *High-resolution TEM. In: Transmission electron microscopy.* 2nd ed. New York: Springer, 2009. p. 483 –506.

[2] JCH Spence, *Experimental high-resolution electron microscopy,* 2nd ed. Oxford U. Press, NY, 1988.

[3] EJ Kirkland, *Advanced computing in electron microscopy*, Plenum Press, New York, 1998.

[4]AF De Jong, D Van Dyck, *Ultimate resolution and information in electron microscopy II. The information limit of transmission electron microscopes.* Ultramicroscopy 49 (1993) 66–80.

[5] R Erni, *High-resolution TEM. In: Aberration-corrected imaging in transmission electron microscopy-An introduction,* 2nd ed. Imperial College Press, London, 2015.

[6] W Jiang and W Chiu, Web-based Simulation for Contrast Transfer Function and Envelope Functions, Microsc. Microanal. 7 (2001) 329–334. https://share.streamlit.io/wjiang/ctfsimulation.

[7] MV Sidorov, ctfExplorer: Interactive software for 1d and 2d calculation and visualization of TEM phase contrast transfer function. Microsc. Microanal. 8s2 (2002)1572 –1573CD. http://www.maxsidorov.com/ctfexplorer/

[8] DRG Mitchell, Contrast transfer function script (2017). http://www.dmscripting.com/contrast_transfer_function.html

[9] S-C Lee, J-M Jeung, S-G Lee and J-G Kim, exCTF simulator: Simulation tool for phase contrast transfer function for aberration corrected transmission electron microscopy, Journal of Analytical Science and Technology 11 (2020) 31.

[10] X-Z Li, Landyne: a software suite for electron diffraction simulation and crystallographic analysis (2022). https://landyne.com

[11] D Shindo and K Hiraga, High-Resolution Electron Microscopy for Materials Science, Springer (1998).

[12] S. Uhlemann, M. Haider, Residual wave aberrations in the first spherical aberration corrected transmission electron microscope, Ultramicroscopy 72 (1998) 109-119.

[13] M Lentzen Progress in Aberration-Corrected High-Resolution Transmission Electron Microscopy Using Hardware Aberration Correction, Microsc. Microanal. 12 (2006) 191–205.

[14] M. O'Keefe, "Resolution" in high-resolution electron microscopy, Ultramicroscopy 47 (1992) 282-297.

[15] Joachim Frank, Detection of Object Movement in the Optical Diffractograms of Electron Micrographs, Optik 30 (1969) 171-178.